PHYSICAL REVIEW D

PARTICLES AND FIELDS

THIRD SERIES, VOL. 4, NO. 3 1 AUGUST 1971

Phenomenology of Muon Showers Underground*

K. H. Davis, S. M. Fall, R. B. Ingebretsen, and R. O. Stenerson

University of Utah, Salt Lake City, Utah, 84112

(Received 12 February 1971)

Measurements of shower arrival directions (incident in a range of zenith angles between 40° and 70° and slant depth of rock between 2×10^5 and 6.5×10^5 g cm^{-2}), structure, and intensities are used as the basis to develop a detailed descriptive phenomenology of muon showers underground. Distributions in right ascension and declination corresponding to minimum values of the median primary energy ranging from 25 TeV for single detected muons to 9000 TeV for events where six muons were detected revealed no compelling evidence for anisotropy in the primary radiation. Measurements of counting rates of groups of two and three of the nearly parallel muons in individual showers as a function of muon separation (structure) were found to be consistent with a shower radial density distribution having the form $\rho(r)=P(r/\sigma)\times\exp(-r/\sigma)$, where r is the distance of the shower axis in m, P is a polynomial in (r/σ), $\sigma=K\times(\sec\theta)^{1.3}/E_\mu^{0.8}$, θ is the zenith angle in degrees, E_μ is the threshold muon energy in units of TeV, and $K=3.6$ m. The empirical shower radial density distribution above reduces to one predicted by Adcock, Wdowczyk, and Wolfendale on the basis of a detailed shower development calculation with a value of $K=4$ m at an energy of 1 TeV and a zenith angle of 45°. Assuming that the distribution of shower sizes is proportional to a power law in shower size, the exponent of the shower-size distribution was measured and found to lie in the range -3.5 to -4.5. The parameters of an empirical density spectrum were optimized by iterative fits to the numbers of events where one to three muons were detected with the result that best-fit parameters were close to those previously obtained by Porter and Stenerson using a smaller sample of shower data. The predicted energy and angular dependence is shown to be in reasonable qualitative agreement with intensities measured in 20-m^2 detectors.

I. INTRODUCTION

In hadron-hadron collisions at energies greater than 30 GeV, the most probable result is that three or more pions will be produced. Such events are a common feature of accelerator scattering experiments at high energies, and violent interactions producing large numbers of secondary particles dominate cosmic-ray observations. The result is common, but these processes are not well understood for the following reason: The events are complex kinematically, and a theoretical base is needed to proceed efficiently with the analysis. A complete understanding will undoubtedly involve the dynamics of strong interactions, which are themselves poorly understood at present.

Although no detailed description of multiparticle final states exists, a number of qualitative, empirical aspects of these processes are known. They deal mainly with the average values of simple observables, like energy and momenta averaged over all production channels. The number of charged secondaries is observed to be a slowly increasing function of the center-of-momentum

energy E_0.[1] The mean energy of the secondaries in the center-of-momentum system is small compared to E_0 and changes slowly with E_0 in a way which is consistent with the energy dependence of the number of secondaries produced.[2] In contrast, a projectile nucleon emerges from the collision retaining a large fraction of its initial laboratory energy.[3] The average value of the transverse momenta for all particles is a fraction of a GeV/c and probably increases slowly with E_0.[2,4,5] Angular distributions of all secondary particles are observed to peak both forward and backward in the center-of-momentum system.[2] At accelerator energies, the secondaries produced are known to be predominantly pions, but at cosmic-ray energies, the ratio of kaons to pions is commonly taken to be 0.2 or larger.[6-9]

Cosmic-ray data offer, in principle at least, a means of learning a great deal about production processes involving large numbers of secondary particles. Interactions of energetic primary cosmic radiation initiate huge showers of electrons, photons, and strongly interacting particles which cascade down through the earth's atmosphere. Much of the shower is absorbed by subsequent interactions in the atmosphere, and what remains of the shower reaching the surface of the earth is quickly absorbed in the earth, with the exception of neutrinos and the muon core of the air shower. The muon cores of air showers appear deep underground as nearly parallel bundles of muons passing simultaneously through charged particle detectors.

The high energies of the primary cosmic radiation, plus the fact that interactions of the primaries and of the secondaries produced by these interactions may be followed through many radiation lengths, make the air-shower phenomena an attractive testing ground for theories of high-energy interactions. In practice, there are many difficulties, low rates and the fact that the interactions of the primaries are not observed directly being chief among them.

In spite of the difficulties, air showers have been vigorously studied, using a variety of experimental techniques at sea level and at mountain and balloon elevations, and useful results have been obtained.[10] The emphasis of the present experiment is on the muon cores of air showers which penetrate to great depths underground. This aspect of air showers has not been extensively investigated until recently[11-13] because of the unavailability of large underground detectors having both the necessary angular and spatial resolution.

The magnetic-tape records generated by the Utah cosmic-ray detector may be analyzed for many types of events. The present work represents one analysis of events selected with a particular goal in view. Studies focusing on the zenith-angle dependence of muons and on the isotropy of arrival directions of muon-producing primaries have been reported, and an analysis of multiple muons using a different approach is under way.[14]

Much of the apparent complexity of muon shower data is due to the geometry of the interactions in the atmosphere, the geometry of the underground muon detectors, and the strong dependence of the measured rates on the slant depth of rock penetrated. The purpose of the present work is to provide the descriptive phenomenology of muon showers underground in terms of empirically derived density spectra, shower-size, and radial density distributions, which are a function only of the zenith angle of shower arrivals and muon threshold energy. The phenomenology provides a means of testing theories of high-energy interactions via a shower development calculation against muon shower data without invoking the complexity of the experimental situation. It is hoped that this work will stimulate further theoretical analysis of the processes which produce high-energy muons observed underground.

II. SHOWER DEVELOPMENT ANALYSES

A. Qualitative Features

Measurements of the density spectrum of the electron component of air showers at the surface of the earth, both accompanied and unaccompanied by muons observed underground, may be used to infer a power-law relation between the number of muons in the shower and the number of electrons. The number of electrons N is in turn related by a power-law dependence to the primary energy. These relations show that the number of muons M is proportional to a power law in the primary energy having an exponent greater than $\frac{1}{2}$. The value of the exponent makes it clear that the muons observed do not all originate in the initial interaction, because the dependence of the number of charged secondaries on primary energy is probably proportional to $E_p^{1/4}$ (or $\ln E_p$) over the range of primary energies covered by the present experiment.[15] But the number of interactions must be small because otherwise the exponent would be close to unity.

The primary energy corresponding to muon showers observed at a given depth has a minimum value which is set by the necessity of producing a muon or muons which can penetrate that depth of earth. When the primary energy is much higher than the minimum value, not only is the frequency of muon showers reduced because of the steepness of the primary energy spectrum, but the probability of the decay of secondaries into muons diminishes.

That the muons observed underground result from interactions occurring near the top of the atmosphere follows from the argument that the number of interactions that the primary makes must be small and that the atmospheric depth is of the order of 1000 g cm^{-2}, while the interaction mean free path for the primary cosmic rays is of the order of 80 g cm^{-2}. Therefore, we expect that the muons observed are produced by interactions occurring at altitudes above 10 km in the first several hundred g cm^{-2} of the atmosphere.

To a first approximation the lateral dimensions of showers observed underground should be proportional to $(\sec\theta)/E_\mu$, where θ is the zenith angle and E_μ is the minimum muon energy required to penetrate a given depth of earth. This result follows from the previous arguments and the fact that the mean transverse momentum of secondaries produced is a fraction of a GeV/c and increases only slowly with primary energy. Actually, the exponent of $\sec\theta$ must be somewhat greater than unity because the vertical depth in the atmosphere from which muons come decreases as θ increases, and the inclined distance to production levels thus increases faster than $\sec\theta$. The exponent of the energy must be somewhat less than unity because the muon energy spectrum has a slope which increases with energy and the ratio of the mean energy to the threshold energy, E_μ, therefore decreases with E_μ.

The radial density distribution is expected to fall off rapidly with distance R from the shower axis because the transverse momentum distribution for secondaries produced in the primary interactions is a rapidly decreasing function of transverse momentum.[16] Compensating for this, in part, and slowing the rate of decrease at large R is the increase in the median height of the point of origin and the decrease in the mean muon energy with increasing R. From the fact that large numbers of secondaries are produced and that the leading nucleon keeps a large portion of its energy, it can be argued that the radial density distribution observed should have radial symmetry. Inasmuch as essentially all muons observed underground are produced in interactions involving large numbers of secondaries, it is reasonable to expect that the shape of the shower radial density distribution will not be a strong function of the number of muons present.

B. Model Approaches

Essentially all model analyses begin by assuming a power-law dependence of the primary energy spectrum and an interaction mean free path of 80 g cm^{-2} for the primary particles. The chief difference is in the next step of the analysis where the distributions that describe the details of individual interaction processes are either taken from extrapolated accelerator measurements or calculated from the primary interaction on the basis of the model. Both approaches must take into account the development of the shower as it propagates through the atmosphere.

The conservative model[17] advanced by the group at the University of Durham, England, takes advantage of the economies in analysis offered by the first approach and makes use of extrapolated accelerator results and distributions obtained from other cosmic-ray experiments. The points of interaction, as well as the energy released in these interactions, are obtained by a Monte Carlo method. The lateral extent of each component of the shower is calculated by tabulating moments of the radial density distributions of the component particles. The conservative-model treatment is especially relevant to the present work because of the detailed treatment of the muon component in the range of energies and zenith angles accessible to the Utah experiment.

Two aspects of the primary interaction that strongly influence muon-shower predictions made using any model are the transverse momentum distribution of secondaries produced and the energy dependence of the mean number of charged secondaries. As a guide to what will be required, we have the distributions of transverse momentum measured in accelerator p-p and π-p scattering experiments (Table I). These results do not resolve the question of shape other than to indicate that the distribution must decrease rapidly with increasing transverse momentum, and that the mean value of the transverse momentum for all secondaries must be a fraction of a GeV/c.[4,16] A combination of accelerator and cosmic-ray results indicates that the best fit to the mean number of charged secondaries varies logarithmically with energy up to 800 GeV.[15]

III. SURVEY OF PREVIOUS EXPERIMENTAL RESULTS FROM UNDERGROUND SHOWER STUDIES

A. The Cayuga Salt Mine Experiments

In the early 1950's, a remarkable series of experiments were carried out in a salt mine near Ithaca, New York.[11] The experiments were remarkable both in conception and in the amount of information that was extracted from a relatively small number of shower events. The experimental apparatus consisted of an array of air shower detectors at the surface operated in coincidence with arrays of lead-shielded detectors 593 m (i.e., 1.574×10^5 g cm^{-2}) underground. It was concluded from these nearly vertical measurements that the

TABLE I. Transverse momentum distributions used in the conservative-model analysis. $N(P_t)$ is the transverse momentum distribution of secondaries produced in accelerator π-p and p-p scattering experiments.

C. K. P.	$N(P_t)=\frac{P_t}{P_0^2}\exp(-P_t/P_0)$
Elbert *et al.*	$N(P_t)=\frac{1}{1.33P_0}\left(\frac{P_t}{P_0}\right)^{3/2}\exp(-P_t/P_0)$
Aly *et al.*	$N(P_t)=\frac{2P_t}{P_0^2}\exp(-P_t^2/P_0)$
Ratner *et al.*	$N(P_t)\propto\exp(-\alpha P_t^2)$

particles detected underground were muons and that practically all showers having more than 500 electrons at the surface contained a muon with a range exceeding the experiment depth. In addition, it was observed that when there were pairs of muons they appeared parallel (within the experimental resolution which varied from 30° to 3° for different cases) and that the air showers associated with these events were on the average much larger than those associated with single muons underground. These results argued that muons observed underground are created by decay processes occurring in the atmosphere. The median primary energies responsible for producing single muons and pairs at the experiment depth were estimated to be 40 and 1000 TeV, respectively.

The distributions of muon shower sizes underground were inferred from the surface measurements of the electron component and from more direct measurements on the muons observed underground. From measurements of electron showers at the surface with and without the associated detection of muons underground, the distributions of showers containing M high-energy muons, $F(M)$, was estimated to be $\propto M^{-4\pm1}$.

The second, more accurate, method made use of the spatial correlations observed in pairs of parallel muons. These correlations indicated that the density of muons is large only within 13 m of the axes of these events. Coulomb scattering, which would be of the order of $\frac{2}{3}$ at the depth of this experiment, and the angles introduced in the decay of either pions or kaons into muons, account for only a small fraction of this width. Assuming that the extent of the showers was due entirely to the angular distribution of secondaries from which the muons underground were produced, it was possible to correlate the measurements where one, two, and three muons were detected in terms of a simply approximated square radial density distribution and power-law shower-size distribution. The ratio of the twofold coincidences to the number of single muons observed tested the form of $F(M)$ for small values of M. The ratio of twofold to threefold coincidences tested the form of $F(M)$ for larger values of M. These conclusions follow from estimates made of the number of muons present when one, two, and three muons were observed. Single muons were estimated to come from showers containing only one to two muons, two-muon events from showers containing two to thirty muons, while three detected muons corresponded to showers containing more than one hundred muons. Assuming that $F(M)$ had a power-law dependence on M as before, both ratios indicated an exponent of M close to −3.4. These results implied that the exponent of the shower-size distribution was not a sensitive function of the number of muons at the experiment depth.

B. The Kolar Gold Mine Experiment

A series of similar experiments with fewer recorded shower events in the early 1960's, carried out in the Kolar Gold Mines in India,[12] also used a surface array of electron detectors, but extended the earlier near-vertical measurements (see Sec. III A) by locating muon detectors at two depths (266 and 590 m, respectively). The frequency of multiple muons was found to be consistent with a mean production height of 10 km, an average transverse momentum of 0.4 to 0.6 GeV/c, and the energy dependence of the integral spectrum of surface muons. Distributions of arrival directions of the showers with high-energy muons in right ascension showed no significant deviation from uniformity.

C. The Silver King Mine Experiment in Utah

With the completion of the Utah cosmic-ray detector in the mid-1960's, it became possible to study muon showers underground incident in a range of zenith angles between 30° and 70° and slant depths of rock between 2×10^5 and 6.5×10^5 g cm^{-2}. In addition, the aperture of the Utah detector was sufficiently large so that enough data might be collected in reasonable running times to study underground muon showers in some detail. The first brief run with the Utah detector showed that these events could be characterized by a shower radius of 6 to 10 m, a multiplicity spectrum which is a power law in multiplicity M having an exponent between −3.4 and −4.0, and no observable anisotropy in the arrival directions of primary cosmic radiation producing the shower events.[13] These data, together with measurements of events containing a single penetrating muon, were used to derive an empirical density function that accounted for the energy and angular dependence of events where one, two, and three muons were detected, as well as the absolute numbers of these

events observed.

Tests of spatial correlations of muon pairs from events where there were only two muons and events where there were three or more muons present showed that the observed radial density distribution was not a sensitive function of the number of shower muons present. The density spectrum derived empirically was compared with the one predicted by the conservative-model analysis[17] of shower development (Sec. II), with the result that there was good agreement between the shapes predicted and derived. The agreement implied that the essential features of the interaction were a mean charged secondary multiplicity which varied with primary energy, E_p, as $E_p^{1/4}$ (or $\approx \ln E_p$) and a mean transverse momentum for the secondaries of 0.4 GeV/c. The results were not inconsistent with a flux of primary cosmic rays consisting of protons only.

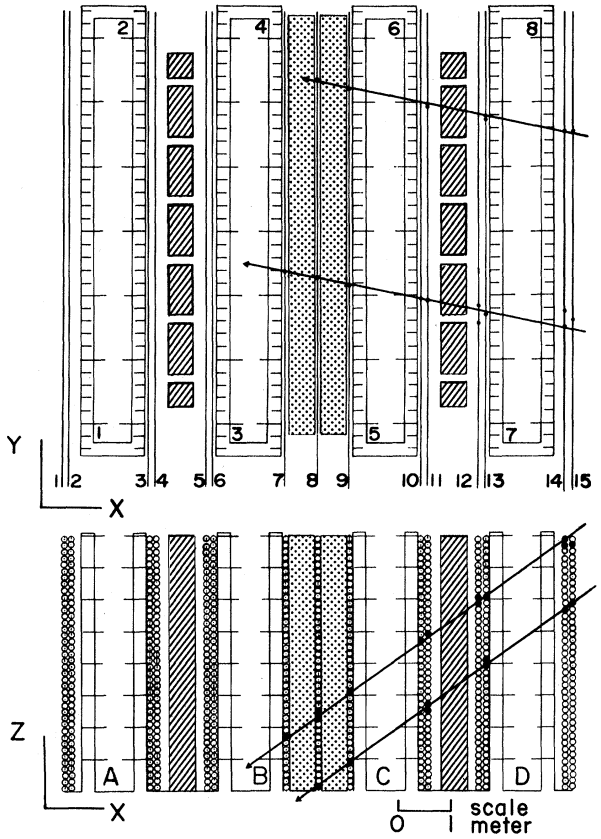

FIG. 1. Front (*XZ* plane) and top (*XY* plane) views of the University of Utah detector. In the front view, cylindrical spark counters are seen end-on as circles stacked in columns 40 high on either side of water-filled Čerenkov tanks labeled *A*, *B*, *C*, *D*. The dark cross-hatched areas between *A* and *B* and between *C* and *D* are the solid iron magnets. The light dotted areas between *B* and *C* are concrete blocks. In the top view, columns of sonic cylindrical spark counters appear as lines labeled 1 to 15, and the light collecting walls of the Čerenkov tanks are labeled 1 to 8. The 7 groups of spark counters are the columns that follow: (1 and 2), (3 and 4), (5 and 6), (7 and 9), (10 and 11), (12 and 13), (14 and 15).

A second experiment, done using three additional small detectors located in a tunnel adjacent to the main Utah detector and triggered by it, made it possible to study pairs of muons in shower events separated by distances as great as 50 m.[18] The results were combined with the counting rates for pairs in the main detector and presented in terms of the counting rate for an equivalent pair of 1-m^2 detectors beneath 2.5×10^5 g cm^{-2} of rock and oriented at a 45° zenith angle. An approximately exponential dependence of the counting rate on the detector separation was observed, which decreased by a factor of $1/e$ in 10 m. These results are consistent with a radial density distribution which falls off somewhat less rapidly than exponentially with distance from the shower axis. Comparison with rates predicted by the conservative-model analysis[17] indicated that the mean value of transverse momentum for the shower muons was $\langle p_t \rangle = 0.6 \pm 0.05$ GeV/c for the corresponding median primary energy of approximately 2×10^5 GeV. The form of the transverse momentum distribution giving the best fit to the experimental data was that proposed by Elbert (see Table I).

In a third experiment,[19] intensities of events having one to three muons in the main detector were studied. Because the probability for seeing an event with a given number of muons depends sensitively on the geometry of the detector, a correction was made to present the data in terms of intensities that would be observed in an omnidirectional detector having a constant area of 20 m^2. Comparisons of these results with the conservative theory again confirmed that the energy dependence of the mean number of charged secondaries on the primary energy, E_p, was proportional to $E_p^{1/4}$ (or $\approx \ln E_p$).

IV. DESCRIPTION OF THE PRESENT EXPERIMENT

The University of Utah detector is located in an underground chamber of the Silver King Mine near Park City, Utah. The chamber lies 1850 ft below the surface of the mountain and three miles into the mountain by way of a horizontal railway through the Spiro Tunnel. The geographic coordinates of the site are 40.623° north latitude, 111.537° west longitude at an elevation of 6950 ft above sea level.

The detector shown in Fig. 1 consists of an array of 600 cylindrical spark counters arranged in 15 vertical planes of 40 counters each, which are triggered by coincidences between pairs of the four water Čerenkov counters. Discharges in the cylin-

drical spark counters are well localized, making it possible to detect the passage of more than one muon through an individual counter. The locations of discharges in the spark counters are recorded each time the detector is triggered on magnetic tape, and a pattern-recognition computer program is used to reconstruct the events from this information.

The amount of rock traversed by muons arriving at the detector from various directions was determined graphically. Topographic maps from the U.S. Geological Survey with 40-ft contour intervals were used to draw profiles of the mountains as seen in vertical cross sections taken through the detector station at various angles. Slant depths obtained from these profiles are estimated to be accurate to ±20 ft.

Handbook values for our local formation of rock based on widely distributed surface samples give an average for the density of 2.47 $g\,cm^{-3}$ as compared with the value of 2.61 $g\,cm^{-3}$ obtained from measurements of samples taken from underground tunnel areas. The best value of the mean density of rock has been taken to be 2.54 $g\,cm^{-3}$. The weighted average of Z^2/A was found to be 5.65 and this value was used to correct our depth values to that of standard rock ($Z^2/A = 5.5$), a correction of 0.5% to 2% over our range of depths. The difference between our best mean value of rock density, the handbook value, and the underground samples is ±2.5%, and it is unlikely that we would have to contend with greater deviations than this. Variations of this size would not affect the main conclusions of this work.

Shower data displayed at fixed zenith and slant depth which show that the measured rates are independent of azimuth within statistical uncertainties argue for the essential uniformity of rock density at the experimental site. Assuming a uniform rock density, threshold muon energies were estimated from the slant depth of rock penetrated, using the range-energy relation of Barrett *et al.* with $b = 3.5 \times 10^{-6}$ $cm^2\,g^{-1}$. The measured rates have roughly the same attenuation with slant depth as do vertical single-muon intensities. This observation is the basis of the correction for the distribution of slant depths in a given depth interval (see Appendix A).

The angular resolution achieved may be estimated by measuring the angle between trajectories of pairs of muons in events where more than two muons are detected. More than $\frac{2}{3}$ of the pairs were seen to be parallel within 1° (see Fig. 2), a result which includes machine resolution, multiple scattering, and angles introduced in the decay processes. These results have been used to argue that the muons observed originate in atmospheric interactions of primary cosmic rays.[13]

Discharges in individual spark counters are located by a sonic ranging technique to a precision of ≈ 3 mm. Additional uncertainty in the position of the muon trajectory is introduced by the geometrical consideration that the counters are 6 in. in diameter. Taking these factors and others into account, the separation between parallel muon trajectories may be estimated to better than 3 in.

The description of the detector and its mode of operation has been deliberately brief. Details of the design, construction, mode of operation and the *in situ* method of determining triggering efficiencies for the cylindrical spark counters and the Čerenkov counters have been discussed elsewhere.[14]

V. ISOTROPY OF THE PRIMARY RADIATION

Individual muons detected in the present experiment have energies of 0.75 TeV or greater so that neither they nor the primary cosmic rays whose interactions produce them are affected by solar or terrestrial magnetic fields.[20] Shower arrival directions, then, accurately reflect the arrival directions of the primaries. Because our observations of muon arrival directions are tied to the rotation of the earth, causing the detector to scan the entire range of right ascension each day, we would expect an isotropic flux of primary cosmic rays to produce a uniform distribution of observed showers in right ascension. Additional complications arise in the case of the present experiment

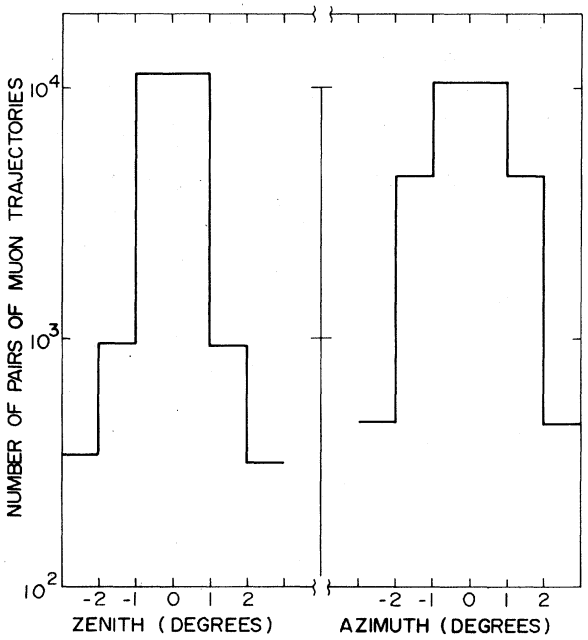

FIG. 2. Zenith and azimuth angular deviations between pairs of muons in individual shower events.

because of the variation of rock depth above the detector and the variation of triggering efficiencies with angle. However, each declination band at a given right ascension can collect data over the entire range of zenith and azimuth (hence, zenith and slant depth) accessible at that declination. These measurements, which make use of continuous complete sidereal days of recorded data, are, then, independent of detector triggering efficiency, topography, and composition of the mountainous overburden. Accordingly, the apertures used in this phase of the measurements were as relaxed as possible. Individual muons were required only to pass through three cylindrical spark-counter groups and one forward (as seen by the incoming muon) Čerenkov wall. The triggering system demands a coincidence between a pair of the four Čerenkov counters, but in the case where more than one muon is present, the requirement may be satisfied by one muon passing through one tank and a second muon passing through another.

For this particular study, a program was developed to take the time of day and the arrival zenith and azimuth angles and convert them to declination and right ascension. Events were sorted into arrays of 360 bins, 10° in declination by 10° in right ascension, extending from declinations 20° below the celestial equator to 80° above it. Constraints imposed by detector triggering requirements prevented collection of data nearer to the celestial poles. Data distributions were compiled for events where one to six muons were detected. Care was taken to use only data from continuous runs of complete sidereal days. All data in a given run were rejected if there was evidence of an electronic system failure in any part of the run.

A. Analysis of Distributions in Right Ascension

The basic analysis consists of displaying the numbers of events at fixed declination as a function of right ascension and comparing these with the average number in each declination band and the 1-standard-deviation limits from the averages (see Fig. 3). Lists of random digits were used to generate distributions in right ascension that had the same number of total counts at each declination as did the recorded data. This was done for several independent sets of random digits with the result that a number of rather intriguing dips and bumps in the real data could be seen to be no greater than would be expected from a random source. The data were also Fourier-analyzed in right ascension and the first ten Fourier sine and cosine coefficients were found to be the same within statistical uncertainties as those generated by the list of random digits. A linear regression was performed on the distributions summed over all declinations for

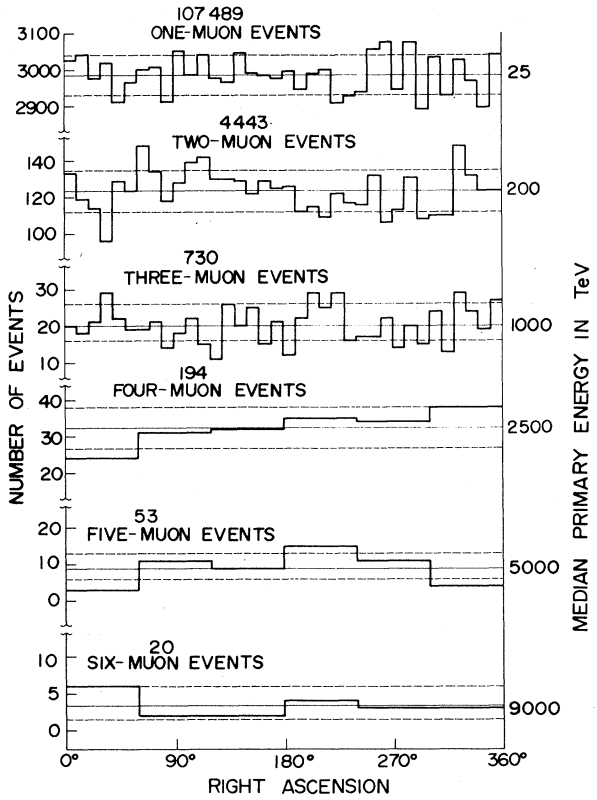

FIG. 3. Distributions of muon-shower arrivals in right ascension for events where one to six muons were detected. Estimates of median energy are from the conservative-model analysis.

showers having one to six muons. The results are shown in Table II. Figure 3 gives estimates of the minimum value of the median primary energy which range from 25 TeV for singles to ≈ 9000 TeV for six-muon events. The linear regression coefficients calculated are not strikingly different from those for random distributions.

The data were divided roughly according to whether they were recorded during the first or second half of the running period and compared

TABLE II. Linear correlation coefficient, R, and the probability that a random distribution would have a linear correlation coefficient as large or larger than R, $P(>R)$, for the right-ascension distributions of events where one to six muons are detected.

Number of detected muons	R	$P(>R)$
1	1.08×10^{-1}	5.3×10^{-1}
2	1.32×10^{-1}	4.41×10^{-1}
3	3.7×10^{-2}	8.3×10^{-1}
4	2.6×10^{-1}	1.3×10^{-1}
5	-1	6×10^{-1}
6	-8	8×10^{-1}

again to distributions generated by random numbers. None of these tests showed any compelling evidence for the existence of an anisotropy.

B. Analysis of Distributions on the Celestial Sphere

We now make use of the results of Sec. V A that the data are nearly uniform in right ascension at all declinations. Binomial statistics were used to compute the fractional standard deviations from the average at each declination (referred to herein as scores) for one- and two-muon events. Although there are different total numbers of events in the ten declination bands, this procedure reduces the 360 elements of each array to a common standard of comparison.

The motivation for displaying the data in this way is to look for broad features whose shape and position might persist in independent blocks of the data. No narrow anisotropies would be expected unless there was a significant flux of energetic neutral primary particles which would be undeflected by galactic magnetic fields. Evidence for neutral primaries at sea level was advanced by Cowan, Ryan, and Buckwalter,[21] but these results were not confirmed in a shallow underground study by Barton, Betts, and Pourgides.[22] Even if energetic primary cosmic rays were trapped by the magnetic fields of the galactic spiral arms,[23] the anisotropy would be a broad one because of the energy distribution of probable cosmic-ray sources (i.e., supernova explosions and pulsars), possible motion of the source relative to the field lines, etc. If the cosmic rays produced in the Galaxy act as an extremely hot and tenuous gas which is only partially constrained by the galactic magnetic field[20] and if cosmic rays are capable of locally inflating this field structure to escape into the galactic halo, then the degree of isotropy is related to the average distance that the cosmic rays travel along the spiral arms before they escape. In this picture, cosmic rays spend most of their time in the weaker magnetic field of the halo. Cosmic rays produced at any point in the Galaxy may return to the spiral arms at any other point. The cosmic-ray flux would then appear even more diffuse. The problem of doing muon astronomy is analogous to the problem of doing optical astronomy through a piece of frosted glass. If one made very sensitive light-detecting instruments, he might arrive at the conclusion that there was a Milky Way.

With these thoughts in mind, isoscore contour maps were made on the celestial sphere. Random number distributions were generated with the same total number of events at each declination and similar maps were made for comparison. Inasmuch as no compelling evidence for broad anisotropies was seen, we simply show equal-area projections of the celestial sphere, showing regions of positive and negative scores (see Fig. 4).

In the distributions of scores for one- and two-muon events, 3-standard-deviation effects are not uncommon, but these results are not evidence of anisotropy. Similar results are obtained for the distributions generated by random numbers. Distributions of scores for one- and two-muon events are shown in Fig. 5.

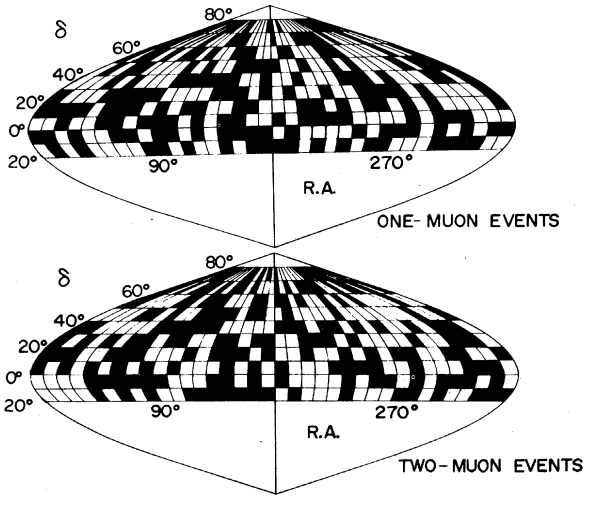

FIG. 4. Equal-area projections of the celestial sphere with positive (indicated in black) and negative (indicated in white) scores for events having one and two detected muons.

VI. SPATIAL CORRELATIONS FOR GROUPS OF TWO AND THREE PARALLEL SHOWER MUONS

A. Probabilities for Groups of Two and Three Muons

Muon showers for the conditions of the present experiment are typically spread over an area of 100 to 300 m^2. Sensitive areas of the Utah detector

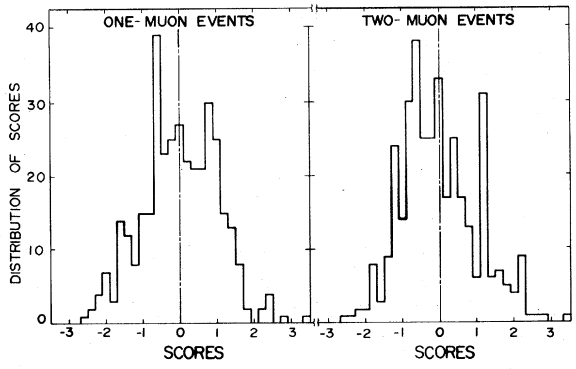

FIG. 5. Distribution of scores for one- and two-muon events.

are less than 80 m^2 and therefore only a fraction of the particles present in a given event are detected. Because the measurements do not fix the position of the shower axis, we cannot directly measure the density distribution of muons in the shower. For this reason, we approach the problem of determining the density distribution in a different manner. Arguments are given in Sec. II that the observed shower-density distribution should have radial symmetry about the shower axis. We assume this to be true and attempt to find a radial density distribution $\rho(R)$ for muon showers which simultaneously predicts the measured rates for pairs, triples, etc., at given separations.

The probabilities for detecting groups of two and three muons can be written down in the limiting case of small detector areas in a straightforward manner as products of independent probabilities. The probability of detecting a single muon in a detector of area A_1 at distance R_1 from the shower axis is $\propto A_1\rho(R_1)$. Hence, the probability of detecting two muons, one in A_1 and another in a detector or area A_2 is $\propto A_1A_2\rho(R_1)\rho(R_2)$, and in a similar way the probability of detecting three muons, one in each of the three detectors, is

$$\propto A_1A_2A_3\rho(R_1)\rho(R_2)\rho(R_3).$$

Results discussed in Sec. III and the physical arguments in Sec. II indicate that the shape of the radial density distribution is insensitive to the number of muons in the shower. Assuming this to be true, the predicted rates of two's and three's will simply be proportional to the distribution of shower sizes, $F(M)$. Specifically, we define $F(M)$ to be the number of showers containing M muons incident in an angular range Ω and a running time T whose axes strike a small area da. Relating the predictions to an actual detector requires an additional multiplicative factor which is the average triggering efficiency, $\langle\epsilon\rangle$.

TABLE III. Triples separation bin analysis.

Combinations	Binned ordered separations	Categories[a]	Combinations	Binned ordered separations	Categories[a]
1[b]	111		29	543	
2[c]	211		30	544	
3	221		31	551	
4	222		32	552	
5	311	2	33	553	
6	321		34	554	
7	322		35	555	
8	331		36	611	1
9	332		37	621	1
10	333		38	622	1
11	411	1	39	631	1
12	421	2	40	632	2
13	422		41	633	
14	431		42	641	2
15	432		43	642	
16	433		44	643	
17	441		45	644	
18	442		46	651	
19	443		47	652	
20	444		48	653	
21	511	1	49	654	
22	521	1	50	655	
23	522	2	51	661	
24	531	2	52	662	
25	532		53	663	
26	533		54	664	4
27	541		55	665	4
28	542		56	666	4

[a]Categories: (1) Cannot satisfy triangle constraint. (2) Linear triangle only. (3) Čerenkov wall requirement impossible. (4) 3 group CSC requirement impossible.

[b]All three separations fall in the range 0 to 2 m.

[c]Two separations in the range 0 to 2 m, one in the range 2 to 4 m, etc.

Combining these arguments gives predicted numbers of pairs at a separation X and predicted numbers of triples at separations of X_1, X_2, and X_3 in a solid angle Ω and a running time T of

$$C_p(X) = \langle \epsilon_p \rangle A_1 A_2 \Omega T N_p \int \rho(R_1)\rho(R_2)da$$

and

$$C_t(X_1, X_2, X_3) = \langle \epsilon_t \rangle A_1 A_2 A_3 \Omega T N_t \int \rho(R_1)\rho(R_2)\rho(R_3)da,$$

respectively. N_p and N_t are functions of M, E_μ, and θ. The integrals are taken over the areas where the shower axes fall and the sums (N_p and N_t) over shower sizes. Specifically,

$$N_p = \sum_M M(M-1)F(M)$$

and

$$N_t = \sum_M M(M-1)(M-2)F(M),$$

where the factors of M multiplying $F(M)$ inside the sum take into account the number of ways that M muons can be chosen to fall one each into sets of two and three counters. We insure the validity of our small-detector approximation by imposing the experimental requirement that the initial subdivision of detector sensitive areas be fine enough (see Sec. VIC) so that two muons are never observed to fall within the same segment of detector sensitive area.

B. Compilation of the Data

In order for a muon to be counted as in aperture, it had to pass through at least one Čerenkov tank and three groups of spark counters. A muon counted as having passed through a Čerenkov detector only if it passed inside a 1-ft border around the forward (as seen by the incoming muon) wall of the tank and passed through the backward wall as well. Every particle present in the event was used to calculate the triggering efficiency of the event; however, only those satisfying the above criteria were counted as being in the allowable aperture.

The basic technique of the study consists of measuring separations in individual shower events between all groups of two and three muons which could, independently of all other particles present, satisfy the triggering and aperture conditions of the detector. In the case of muon pairs, distributions of events in 1-m separation bins are compiled as a function of 2.5° zenith and 5×10^4-g cm^{-2} slant-depth bins ranging from 40° to 70° and 2×10^5 to 6.5×10^5 g cm^{-2}, respectively. The fact that each group of three muons is associated with three separations was an additional complication, and a special binning procedure was adopted. The technique used is as follows: Separations between the muons are calculated and binned according to 2-m separation intervals. The binned separations are then ordered, the largest one first, the next largest second, the smallest third, and the combinations that result are assigned a number ranging from 1 to 56 (see Table III). Distributions of the numbers of events at each combination are compiled then as a function of 5° zenith and 1×10^5-g cm^{-2} slant-depth bins covering the same range as the pair data.

C. Displaying the Data in a Manner Independent of Detector Geometry

We must now take into account the fact that our detector is a large detector while the equations that we have developed in Sec. VI A are for small detectors. What we do in effect is to reduce our large detector to the small-detector approximation by subdividing the detector sensitive area. We compile the sums of products of all small areas, A_1 and A_2, as a function of 1-m separation bins, zenith and azimuth, such that two muons passing one through each of these areas could, independently of all others, satisfy the imposed aperture requirements of the detector. In a similar way, we compile the distributions of the sums of the products of three small areas, A_1, A_2, and A_3, which if three muons passed one through each of these areas, would satisfy the triggering and aperture requirements of the detector.

To make the distribution of these geometrical factors correspond to the binning of the data and the efficiency arrays, we need to convert them from arrays which are functions of zenith and azimuth to ones which are functions of zenith and slant depth. This is done by combining all the distributions at fixed zenith which correspond to the same depth bin. The dependence of the measured rates on depth is strong and we must take into account the distribution of depths contributing to each depth bin. The correction used (see Appendix A) depends on the observations (see Sec. IV) that the measured rates are insensitive to variation in azimuth at fixed zenith and slant depth and that the rates at fixed zenith, but varying slant depth, are attenuated with depth in roughly the same way as are vertical single-muon intensities.

The data could then be cast in the form of rates, which are independent of detector geometry and triggering efficiency, by dividing the numbers of events by the products of areas, average efficiency, solid angle, and time. Hence, in terms of the previous notation, the rates for pairs, R_p, and triples, R_t, are $R_p = C_p/\langle \epsilon_p \rangle A_1 A_2 \Omega T$ and $R_t = C_t/\langle \epsilon_t \rangle A_1 A_2 A_3 \times \Omega T$. The dimensions of R_p and R_t are (number of pairs/m^4 sr sec) and (number of triples/m^6 sr sec), respectively.

The counting rate for a pair of detectors as a

function of separation decreases smoothly with separation (Fig. 6). The rates for triples, however, have a much more complicated appearance (Fig. 7). Most of the apparent structure in the rates of triples is a direct result of the binning procedure. The rates are not continuous because they are combinations of binned, ordered separations, and some of the combinations are not able to satisfy the triangle requirement (see Table III). The justification for introducing this complexity is that it enables us to represent the measurement of a quantity which has magnitude and three separations in a two-dimensional display and, at the same time, not give up any information inherent in the data.

D. Correlation Integrals

The shapes of the predicted distributions of pairs and triples as a function of separation were determined by calculating the following integrals numerically for pairs and triples, respectively:

$$I_p = \int \rho(R_1)\rho(R_2)da \quad \text{and} \quad I_t = \int \rho(R_1)\rho(R_2)\rho(R_3)da.$$

The assumption that these integrals give the shape independent of shower size is consistent with the physical arguments of Sec. II, and the experimental evidence presented in Sec. III to the effect that ρ will not be a sensitive function of M. The factors multiplying these integrals which are functions of θ, E_μ (or, equivalently, slant depth of rock, h), and M control only the magnitude of the rates R_p and R_t.

In evaluating these integrals, it was assumed that the shower axes are uniformly distributed. This task was made much easier by the fact that we had reduced the data taken in our large detector to those equivalent to data taken with small detectors. Hence, we concern ourselves with the response of a group of two and a group of three small detectors in a plane. These integrals of products of normalized distributions (i.e., $\int \rho\, da = 1$) were

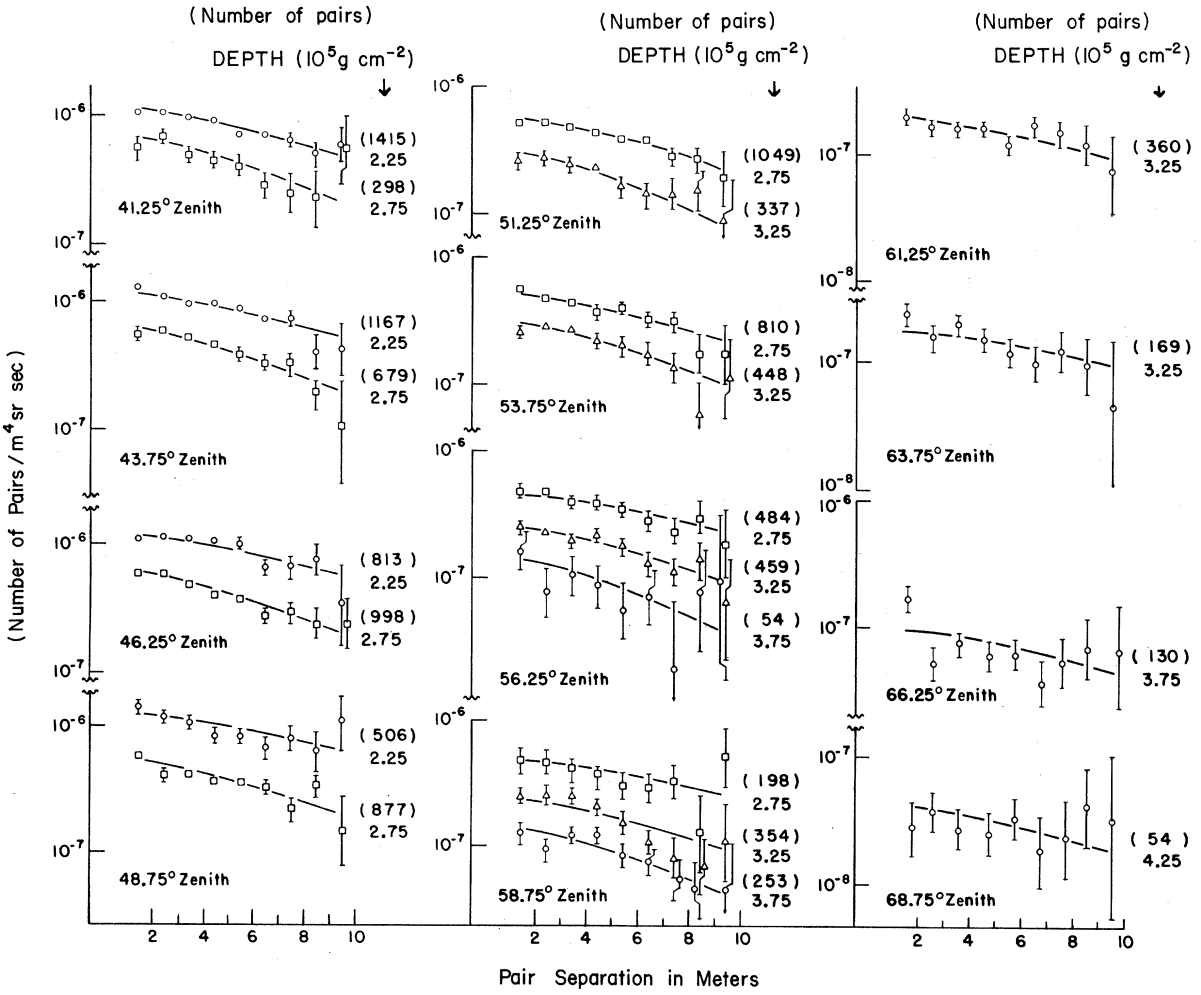

FIG. 6. Counting rates for pairs as a function of pair separation, zenith, and slant depth. Solid lines are the predictions of the optimized radial density distribution (Sec. VI) with K = 3.6 m.

evaluated numerically as a function of the parameter σ of the radial density distribution.

The data of the present experiment provide information on the distributions of pairs of muons having separations as great as 11 m. The characteristic shower radius σ for the range of zenith angles and slant depths accessible to the present experiment is of the order of 5 m. The value may be somewhat larger or smaller depending on the shape of the particular radial density distribution chosen to fit the data and on the particular zenith angle and slant depth. The important point is, however, that σ is comparable to the range of separations accessible, so that the present experiment will not serve to provide a sensitive measurement of the shape of the radial density distribution. In addition, the range of the slant depths accessible at particular zenith angles is small, limiting the precision to which the energy and angular dependence of the characteristic shower radius can be determined. For these reasons and others, a less direct analysis of the data was made by testing the measurements for consistency with reasonable theoretical predictions.

The physical arguments given in Sec. II lead us to expect that the radial density distribution is a steeply falling function of separation from the shower axis, but that the rate of decrease slows at large distances. In addition, these arguments indicate that σ is proportional to a power of $\sec\theta$ greater than unity and inversely proportional to a power of threshold muon energy which is somewhat less than unity.

The shape of radial density distribution inferred from muon pairs at large separations[18] was found to be consistent with the shape of the radial density distribution predicted by the conservative model, having the character required by our arguments above. The conservative model[17] further predicts that $\sigma \propto (\sec\theta)^{1.3}/E_\mu{}^{0.8}$.

We assume that the characteristic shower radius can be expressed as follows: $\sigma = K(\sec\theta)^{1.3}/E_\mu{}^{0.8}$, and parametrize the shape of the radial density distribution predicted by the conservative model as

$$\rho(R) = P(R/\sigma)\exp(-R/\sigma),$$

where

$$\begin{aligned} P(R/\sigma) = {} & (3.7988991\times10^{-2}) \\ & +(-2.7728861\times10^{-2})(R/\sigma) \\ & +(1.3724899\times10^{-2})(R/\sigma)^2 \\ & +(-3.7617982\times10^{-3})(R/\sigma)^3 \\ & +(5.7263392\times10^{-4})(R/\sigma)^4 \\ & +(-4.4695767\times10^{-5})(R/\sigma)^5 \\ & +(1.4005871\times10^{-6})(R/\sigma)^6. \end{aligned}$$

The parametrization might have equally well been achieved in other ways. The one used is adequate for the purposes of the present analysis, being a smoothly varying, well-behaved (positive) function of zenith angle and energy for zeniths ranging from 0 to 85° and energies ranging from 1 GeV to 1000 TeV. The above expression reduces to the prediction of the conservative model for a zenith of 45° and an energy of 1 TeV if K is taken to be equal to 4 m.

The first part of the consistency test involves fitting data in each individual zenith and slant-depth bin to determine the optimum choice of σ (referred to herein as unconstrained fits). Fits were made to pairs only for those zenith and slant-depth bins where there were data in nine consecutive separation bins between 1–2 m and 10–11 m. The criteria for triples were greatly relaxed and fits were made to any bin where data were available at four or more points. From these fits, we see that the values of σ obtained (see Tables IV and V) behave qualitatively in the way that we would expect. At fixed depth as a function of increasing θ, we observe that σ tends to increase. This is simply a reflection of the fact that as the zenith angles increase, the point of origin of the shower particles becomes further away, allowing the showers to spread out over a larger area. For a fixed value of zenith angle as slant depth increases, we see that σ tends to decrease, reflecting the fact that more energetic muons produce an increasingly

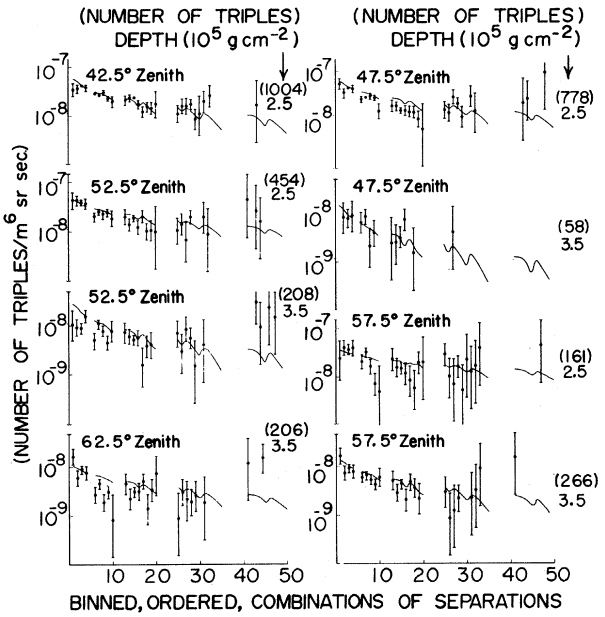

FIG. 7. Counting rates for triples as a function of binned, ordered combinations of separations, zenith, and slant depth. Solid lines are the predictions of the optimized radial density distribution (Sec. VI) with $K = 3.6$ m.

TABLE IV. Distributions in zenith and slant depth of the characteristic shower radius, σ, χ^2_ν, and the normalization constant for (a) the unconstrained and (b) the optimized (with $K = 3.6$ m) fits of Sec. VI to the pair data. When three values of σ and the normalization constant appear in the table, the upper and lower entries were obtained in the fitting process where $\chi^2_\nu = 1$.

(a) Pairs: unconstrained fit

Zenith (deg) \ Slant depth (10^5 g cm^{-2})	χ^2_ν (sum 15.7)					σ (m)					N_p (10^{-4} m^{-2} sr^{-1} sec^{-1})				
	2.25	2.75	3.25	3.75	4.25	2.25	2.75	3.25	3.75	4.25	2.25	2.75	3.25	3.75	4.25
41.25	).52	0.76				6.8	4.8				8.08	2.6			
						5.6					6.0				
						4.8					4.85				
43.75	).86	0.54				6.0	5.8				6.44	2.92			
						5.4	4.6				5.6	2.2			
						4.8	4.0				4.76	1.75			
46.25	1.16	0.56				5.8	5.4				6.6	2.70			
							4.6					2.2			
							4.0					1.80			
48.75	1.50	1.33				6.0	5.8				8.0	2.9			
51.25		0.42	0.27				7.4	8.2				4.20	2.39		
							5.8	5.0				2.9	1.1		
							4.8	3.6				2.21	0.75		
53.75		0.57	0.80				6.8	5.8				3.42	1.44		
							5.4	4.8				2.4	1.1		
							4.4	4.2				1.82	0.92		
56.25		0.20	0.40	0.37			8.8	7.6	4.6			5.00	1.93	0.5	
							5.6	5.2				2.5	1.1		
							4.0	4.0				1.56	0.77		
58.75		0.47	0.54	0.80			6.0	5.2	7.2			2.8	1.02	0.89	
								4.0	5.4				0.7	0.6	
								3.4	4.4				0.61	0.44	
61.25			0.63					8.4					2.0		
63.75			0.43					4.6					0.7		
66.25				2.35					6.8					0.7	
68.75					0.19					9.8					0.6

(b) Pairs: optimized fit with $K = 3.6$ m

Zenith (deg) \ Slant depth (10^5 g cm^{-2})	χ^2_ν (sum 18.1)					σ (m)					N_p (10^{-4} m^{-2} sr^{-1} sec^{-1})				
	2.25	2.75	3.25	3.75	4.25	2.25	2.75	3.25	3.75	4.25	2.25	2.75	3.25	3.75	4.25
41.25	0.52	0.82				5.8	4.4				6.26	2.31			
43.75	1.03	0.55				6.1	4.6				6.59	2.11			
46.25	1.22	0.62				6.4	4.9				7.67	2.33			
48.75	1.62	1.48				6.8	5.2				9.76	2.42			
51.25		0.48	0.34				5.5	4.4				2.69	0.95		
53.75		0.68	0.80				6.0	4.8				2.78	1.08		
56.25		0.33	0.40	0.38			6.5	5.2	4.2			3.04	1.07	0.41	
58.75		0.52	1.26	0.88			7.1	5.6	4.6			3.61	1.15	0.46	
61.25			0.86					6.2					1.22		
63.75			0.68					6.9					1.34		
66.25				2.34					6.4					0.64	
68.75					0.31					6.0					0.25

tightly collimated shower.

Assuming the energy and angular dependence of σ predicted by the conservative model, the data were next iteratively fit with a series of values of K to determine the value of K, giving the over-all minimum χ^2. The results from the fits to the pairs were that $K = 3.6 \pm 0.4$ m, consistent with the predictions of the conservative model. Optimizing the fits to the triples results in a minimum χ^2 that occurs at roughly the same value of K. The distribution of χ^2 vs K is, however, much broader, and the triples may be considered to yield only supporting evidence. The values of K which optimize the fit over-all to the data yield a χ^2 in each case which is not significantly larger than the χ^2 obtained from the unconstrained fits to the data (see Tables IV and V). The rates predicted by the optimized radial density distribution with $K = 3.6$ m are shown superimposed on the data in Figs. 6 and 7. Dividing the pairs data into events where only two muons were observed and events where more than two muons were observed yields similar results, but the statistical uncertainties are larger. All of these results argue that a radial density distribution having the shape and energy dependence predicted by the conservative model is consistent with the measurements of the spatial correlations of pairs and triples of the present experiment.

E. Distribution of Shower Sizes

To obtain the distribution of muon shower sizes underground, we make use of the measured normalization constant, N_p, for pairs and the single muon intensities, I_s, measured for the same zenith and depth bins[19] (see Fig. 8). By definition, the ratio of N_p to I_s is given by $N_p/I_s = \sum_M M(M-1)F(M)/\sum_M MF(M)$. Assuming that $F(M) \propto M^{-\delta}$, the ratio above may be used to estimate δ as a function of θ and h. The motivation for choosing a power-law dependence for the shower-size distribution is given in Sec. II.

Values of δ estimated using unconstrained fits to

TABLE V. Distributions in zenith and slant depth of the characteristic shower radius, σ, χ^2_ν, and the normalization constant for (a) the unconstrained and (b) the optimized (with $K = 3.6$ m) fits of Sec. VI to the triples data. When three values of σ and the normalization constant appear in the table, the upper and lower entries were obtained in the fitting process where $\chi^2_\nu = 1$.

(a) Triples: unconstrained fit

Zenith (deg) \ Slant depth (10^5 g cm^{-2})	χ^2_ν (sum 11.7) 2.5	3.5	4.5	σ (m) 2.5	3.5	4.5	N_t (10^{-3} m^{-2} sr^{-1} sec^{-1}) 2.4	3.5	4.5
42.5	0.73			8			16.8		
				6			7.0		
				5			4.26		
47.5	3.25	0.31		7	5		14.0	0.81	
52.5	0.75	1.99		9	9		24.6	10.0	
				6			7.0		
				5			4.24		
57.5	1.01	0.72		5	8		4.0	4.12	
					5			1.0	
					4			6.54	
62.5		2.90			9			5.5	

(b) Triples: optimized fit with $K = 3.6$ m

Zenith (deg) \ Slant depth (10^5 g cm^{-2})	χ^2_ν (sum 12.7) 2.5	3.5	4.5	σ (m) 2.5	3.5	4.5	N_t (10^{-3} m^{-2} sr^{-1} sec^{-1}) 2.5	3.5	4.5
42.5	0.98			5.1			4.5		
47.5	3.07	0.35		5.8	3.6		7.6	0.35	
52.5	0.76	2.76		6.6	4.2		9.2	0.99	
57.5	1.07	0.72		7.8	4.9		14.3	0.96	
62.5		3.00			6.0			1.5	

pair data in individual slant-depth and zenith bins and those obtained using the optimized fit to the total pair data (see Sec. VI D) with $K = 3.6$ m are given in Table VI. The results are similar, but δ's estimated using the optimized fit to the pairs are more regular functions of θ and h. Both estimates range from ≈ 3.5 to 4.5, in agreement with the qualitative arguments of Sec. II and the previous experimental results discussed in Sec. III. The uncertainties in the values of δ from the unconstrained fits may be estimated by using the measured values of N_p at the 33% confidence level. Accordingly, these were assigned only in cases where the minimum reduced χ^2 was less than unity and the distribution of χ^2 vs σ has a well-defined minimum.

The pair data used in the present analysis are drawn from events where two or more muons are detected so that our results do not refer exclusively to events where one and two muons are observed. On the basis of the arguments in Sec. II, we would not expect δ to depend sensitively on M.

To test the dependence of δ on larger mean values of M, we use the ratio

$$N_t/N_p = \sum_M M(M-1)(M-2)F(M) / \sum_M M(M-1)F(M),$$

assuming as before that $F(M) \propto M^{-\delta}$. Data consisting of 13 511 pairs and 3230 triples were scaled using the measured attenuation of single muons with depth and the behavior of the correlation integrals (Sec. VI D) as a function of zenith angle and energy in the manner of Appendix A to obtain rates at 2.5×10^5 g cm^{-2} and a zenith of 45°. These rate curves yielded $N_t/N_p = 19.2$ corresponding to $\delta \approx 3.7$, which was in agreement with the estimates based on the ratio N_p/I_s and, thus, confirmed the expected insensitivity of δ to M.

VII. DENSITY SPECTRUM PREDICTIONS

Although the function we are deriving is empirical, we construct it in a manner which is strongly

TABLE VI. Distributions in zenith and slant depth of the exponent of the shower-size distribution, δ, for the unconstrained and optimized (with $K = 3.6$ m) fits of Sec. VI to the pair data.

Zenith (deg) \ Slant depth (10^5 g cm^{-2})	Unconstrained fits					Optimized fits ($K = 3.6$ m)				
	2.25	2.75	3.25	3.75	4.25	2.25	2.75	3.25	3.75	4.25
41.25	3.61 3.78 3.89					3.74				
43.75	3.74 3.82 3.92	3.76 3.92 4.07				3.73	3.94			
46.25		3.81 3.94 4.07				3.69	3.89			
48.75						3.60	3.90			
51.25		3.64 3.82 4.01	3.53 3.94 4.21				3.89	4.04		
53.75		3.77 3.98 4.16	3.79 3.95 4.08				3.89	3.97		
56.25		3.61 4.01 4.34	3.68 3.98 4.24				3.87	3.95	4.22	
58.75			4.09 4.36 4.50	3.70 3.97 4.15			3.76	4.02	4.13	
61.25								4.00		
63.75								3.95		
66.25									3.97	
68.75										4.2

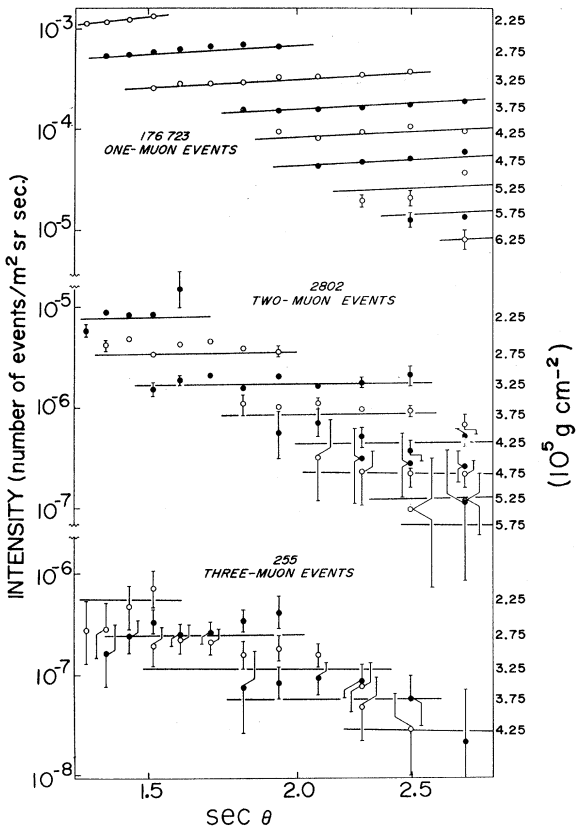

FIG. 8. Intensities for one-, two-, and three-muon events adjusted to standard conditions of a 20-m^2 detector compared to the predictions of the optimized density spectrum (Sec. VIIB) for the same conditions.

guided by physical considerations. The density spectrum developed is required to express the energy and zenith-angle dependence of muon showers as well as the distribution of densities of these showers. In particular, it is constrained when used to predict the number of single-muon events to reduce to the same dependence on depth as the measured single-muon vertical intensities at 0° zenith.[13]

Measured integral electron-density spectra in extensive air showers have the following qualitative character: At low densities, the shape of the density spectrum approaches a power law in density Δ. As the density increases, the density spectrum gradually steepens and again approaches a power law in Δ at the highest densities. It may be argued on general grounds (see Sec. II) that the integral density spectrum of muon showers should have a similar form, and, in fact, detailed development calculations with the conservative model discussed in Sec. III have shown this to be the case.

As regards observations in detectors of moderate size, for $E_\mu > 1$ TeV, further qualitative observations may be made. The region of shower densities which produce single detected muons is very broad, extending downward from densities of 10^{-2} m^{-2} to densities less than 10^{-9} m^{-2} with median densities of $\approx 10^{-4}$ to 10^{-3} m^{-2}. Events where more than one muon is detected come from regions of increasingly higher density; the median shower densities producing two and three detected muons are $\approx 10^{-2}$ m^{-2} and 4×10^{-2} m^{-2} while four- and five-muon events correspond to shower densities which are $>10^{-1}$ m^{-2}. Moreover, the region of densities contributing to observed events of a given multiplicity (i.e., numbers of detected muons) becomes narrower and overlaps the regions contributing to adjacent multiplicities more as the multiplicity increases.

The major shortcoming of the density-spectrum approach is that the shower density must be constant across the detector sensitive area in order that the probabilities have a Poisson distribution. This requirement limits the use of the density-spectrum technique to areas which are small compared to the radial extent of muon showers. The detector sensitive areas in the present analysis (see Sec. VII A) range in size from a fraction of a square meter at the smallest zenith angles to almost 56 m^2 at the largest. Muon showers for the conditions of the present experiment (see Sec. VI D) have an extent of ≈ 100 to 300 m^2 so that the detector sensitive areas are in no case large compared to the shower size. A further approximation made is that the exponent of the power-law dependence on Δ is independent of slant depth. It is more likely that the exponent of the density spectrum should have a mild (i.e., logarithmic) dependence on slant depth, but this may not be an important consideration over the range of depths spanned by the present measurements.

A. Apertures for the Empirical Fits

In determining empirical representations by fitting the data, it is absolutely imperative that no systematic errors be introduced by the aperture chosen. Accordingly, the same aperture requirements are imposed on events of all multiplicities. This is a very severe requirement and one which greatly reduces the number of higher-multiplicity events. We require, then, that every muon trajectory included be able to satisfy the triggering and aperture requirements that a single detected muon must satisfy, which are that each muon pass through two forward Čerenkov walls and their preceding backward walls, as well as three groups of cylindrical spark counters (see Fig. 1). The data were binned in arrays of 2.5° zenith angle, ranging from 40° to 70°, and 5×10^4 g cm^{-2} slant depth, ranging from 2×10^5 to 6.5×10^5 g cm^{-2}.

B. Optimizing Density Spectrum Parameters

The present work is an extension of that done earlier by Porter and Stenerson,[13] who approximated the general character of the differential density spectrum by two intersecting power laws in density. Their density spectrum was of the form

$$\kappa(h, \theta, \Delta)d\Delta = G(h)H(\Delta, \theta)d\Delta,$$

where

$$G(h) = [\exp(bh) - 1]^{-\gamma}$$

with

$$b = 3.5\times10^{-6}\ \text{cm}^2\,\text{g}^{-1},\quad \gamma = 2.4 + 0.25\ln(h/10^5\,\text{g cm}^{-2}),$$

and

$$H(\Delta, \theta) = K_\beta \Delta^{-\beta} \quad \text{when} \quad \Delta > \Delta_0,$$

and

$$H(\Delta, \theta) = K_\alpha \Delta^{-\alpha} \quad \text{when} \quad \Delta < \Delta_0.$$

G is a function having the same dependence on depth as do the measured vertical-muon-depth intensities.[13] H approximates the power-law dependence on Δ of the shower-density spectrum. In these functions, h is the slant depth of rock in g cm^{-2}, θ is the zenith angle in degrees, and Δ is the shower density in m^{-2}. The point of intersection Δ_0 was determined by the relation

$$\Delta_0 = D + E\cos\theta\ \text{m}^{-2}.$$

The starting point of the present analysis is the density spectrum above. Numbers of events having n muons, E_n, detected in running time T, a detector sensitive area S, and a solid angle $d\Omega$ were calculated numerically in each azimuth and zenith bin using the expression below:

$$E_n = \int_\Omega \int_\Delta P_n(\Delta S)\kappa(h, \theta, \Delta)d\Delta d\Omega\, T,$$

where P_n is the Poisson probability distribution; i.e.,

$$P_n(\Delta S) = [(\Delta S)^n/n!]\exp(-\Delta S).$$

The arrays of predicted numbers of events as a function of azimuth and zenith were rebinned in terms of zenith and slant depth, and these results compared with the measured numbers of events corrected by detector triggering efficiency. This process was iterated in the manner described by Porter and Stenerson[13] to obtain parameters for the density spectrum which minimize the χ^2 between the predicted and observed numbers. The set of parameters giving the best fit is the following:

$$\alpha = 1.74,\quad \beta = 3.01,\quad D = 2.33\times10^{-4},$$

$$E = 6.58\times10^{-4},\quad K_\beta = 2.68\times10^{-7}.$$

These parameters are close to the ones previously obtained by Porter and Stenerson,[13] and the differences may be attributed to the larger sample of data in the present experiment. Comparison between prediction and data in individual zenith and depth bins reveals enough irregularity in the data to force the conclusion that systematic errors of unknown origins are sometimes large compared to statistical uncertainties. Accordingly, a numerical estimate of the goodness of fit would have little meaning.

While the total predicted numbers of one-, two-, and three-muon events are in close agreement with the numbers observed, too many four- and five-muon events are predicted (see Table VII). Inasmuch as these are preferentially produced from regions of high shower density, there is the possibility that better agreement might be achieved by altering the shape of the density spectrum in the high-density region. No detailed information about the shape of the density spectrum in this high-density region can be obtained because of the small numbers of four- and five-muon events observed. We can, however, get a rough idea of what will be required by a straightforward extension of the techniques we have developed. Assume for these purposes that the differential density spectrum may be represented by three power laws in Δ – hence,

$$H(\theta, \Delta) = K_\alpha \Delta^{-\alpha} \text{ when } \Delta < \Delta_1,$$

$$H(\theta, \Delta) = K_\beta \Delta^{-\beta} \text{ when } \Delta_1 < \Delta < \Delta_2,$$

and

$$H(\Delta, \theta) = K_\gamma \Delta^{-\gamma} \text{ when } \Delta > \Delta_2.$$

If we arbitrarily require that the total predicted numbers of events of each multiplicity differ by no more than 30% from the numbers observed, then it is possible to show that the parameters of the three-power density spectrum have the following bounds:

$$\alpha \sim 1.74,\quad 2.9 < \beta < 3.0,\quad 5.5 < \gamma < 7.5,$$

$$\Delta_1 \sim (2.23 + 6.58\cos\theta)\times10^{-4}\ \text{m}^{-2},$$

$$0.02\ \text{m}^{-2} < \Delta_2 < 0.03\ \text{m}^{-2}.$$

TABLE VII. Prediction of the numbers of events where one to five muons are detected for the optimized two-power-law density spectrum (Sec. VII B). Comparison is made to observed numbers of events corrected for detector triggering efficiency.

Number of detected muons	Number of events observed corrected for detector triggering efficiency	Number predicted by density spectrum
1	3.27×10^5	3.27×10^5
2	3.15×10^3	3.15×10^3
3	2.60×10^2	2.60×10^2
4	3.40×10^1	6.4×10^1
5	6.00×10^0	2.8×10^1

All combinations of these parameters within the ranges given above were considered and the extremes of the corresponding integral density spectra are compared with the integral density spectrum obtained from the two-power-law representation in Fig. 9 for zenith angles of 0° and 60° and a rock depth of 2.5×10^5 g cm^{-2} ($E_\mu \sim 1$ TeV).

C. Predictions for a 20-m^2 Detector

The optimized two-power-law differential density spectrum discussed in Sec. VII B may now be used to predict the intensities of events where one, two, and three muons are detected in a hypothetical detector that presents a constant sensitive area of 20 m^2 at all zenith angles and slant depths. The advantage of doing this is that the angular and depth dependences are clearly displayed. The predictions are shown superimposed on the data of Cannon and Stenerson[19] in Fig. 8 which were corrected to these conditions by a technique developed by the Durham group.[16] The technique uses the shower radial density distribution predicted by the conservative model (Sec. II) to estimate the probability that a given number of muons will be detected in a detector of a particular sensitive area and correct the observed rates to the standard conditions of a 20-m^2 detector. The predictions of the density spectrum of the magnitude as well as the dependence of the intensities on zenith angle and rock depth are in reasonable qualitative agreement with the measurements over the range of zenith angles and depths accessible to the present experiment.

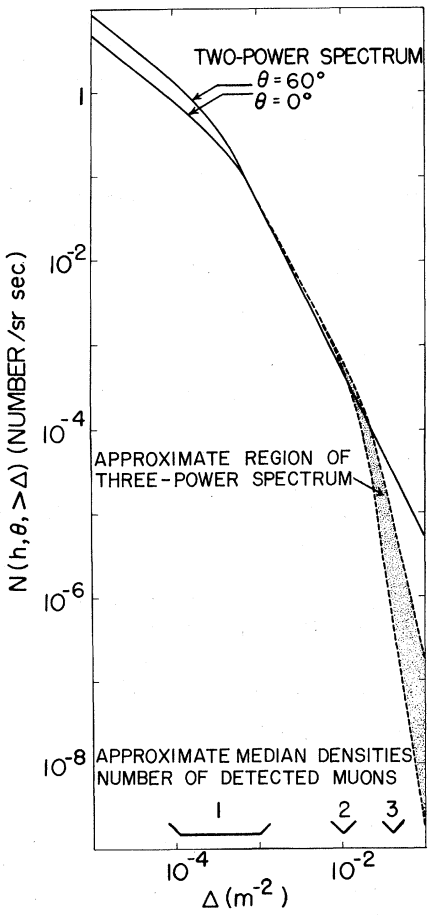

FIG. 9. The integral density spectrum (from the two-power differential density spectrum, optimized for prediction of one-, two-, and three-muon events, Sec. VII B) at 0° and 60° zenith and a slant depth of 2.5×10^5 g cm^{-2} ($E_\mu \sim 1$ TeV). Indicated by dashed lines and shading is the approximate range of an integral spectrum corresponding to a three-slope density spectrum which is constrained to predict total numbers of one-, two-, three-, four-, and five-muon events which are no more than 30% different than the observed numbers. The low-density region which introduces the zenith angular dependence into the single-muon data is virtually the same in either integral spectrum.

VIII. DATA SUMMARY

The data of the present experiment are more extensive than in any previous study of muon showers underground. The isotropy of muon shower arrival directions over a range of median primary energies form 25 to 9000 TeV is tested by a run of 97 days of continuous sidereal time and a sample of 112 929 events. The shape of the radial density distribution and the consistency of the energy and angular dependence of the shape with the predictions of the conservative model are tested by a sample of 12 378 muon pairs and 3228 triples. The empirical fits to the density spectrum are based on a sample of 179 820 events through the highly restricted single-muon aperture. The over-all running time of the experiment was 18 509 814 sec.

IX. CONCLUSIONS

The problem of deriving a descriptive phenomenology of muon showers from measurements on muon showers underground is that no facet of the phenomenology is truly uncoupled from any other. Our approach to the problem has been the following:

The isotropy of the primary cosmic-ray flux producing showers over the range of zenith angles and slant depths accessible to the present experiment was studied by displaying shower arrival directions in celestial coordinates. Measurements on the counting rate of muon pairs extending to separations as great as 50 m provided a test of the shape of the shower radial density distribution. The energy and angular dependence of the mean shower radius which were estimated from physical arguments and from detailed shower development calculations, were tested for consistency against the counting rates for groups of two and three muons

as a function of separation. From the ratio of the normalization constants for the counting rate of pairs to the single-muon intensities measured in the same depth-angle bins, we estimate the exponent δ of the power-law dependence of the shower-size distribution. We test the dependence of δ on shower size M by comparing these estimates of δ with that obtained from the ratio of the total triple-muon rates to the total muon-pair rate. We test the dependence of the shape of radial density distribution on shower size by measuring counting rates for pairs of muons in events where only two muons are observed and events where more than two muons are observed. Parameters of the density spectrum were optimized by fitting the measured numbers of events where 1 to 5 muons were detected. The radial density distribution, the exponent of the shower-size distribution, and the density spectrum so derived are functions of zenith and slant depth only.

The empirical representations developed were strongly motivated by the physical arguments and by the results of detailed shower development analysis based on the conservative model. Predictions made using these representations are in reasonable qualitative agreement with these and other available data. All of these results argue that the derived shower-size distribution, radial density distribution, and density spectrum provide a consistent phenomenological representation of muon showers underground over the range of zenith angles and slant depths currently accessible to experiment.

APPENDIX A

Consider the distributions of the geometrical factors A_1A_2 and $A_1A_2A_3$ for particular separations in the zenith bin J and the azimuth bin L. We factor the strongest part of the depth dependence from N (i.e., N_p or N_t) letting

$$N(J, h\to L) = I_v(h\to L)n(J, h\to L),$$

where I_v is a smooth fit to the vertical depth intensity for single muons,[13] and n is found empirically to be a weak function of slant depth. Here, the notation $h\to L$ is to be read "at the slant depth h corresponding to the azimuth bin L." Then

$$N(J, h\to L) = [I_v(h\to L)/I_v(K)]\, I_v(K)n(J, h\to L).$$

$I_v(K)$ refers to the intensity evaluated at the center of the depth bin K. Then, over the small range of depths in a single-depth bin,

$$N(J, h\to L) \approx [I_v(h\to L)/I_v(K)]\, I_v(K)n(J, K)$$

$$= [I_v(h\to L)/I_v(K)]\, N(J, K).$$

Using these results and the expression giving the predicted number of pairs in Sec. VI yields

$$C_p(J, K) = \langle \epsilon_p(J, K)\rangle \sum_L [I_v(h\to L)/I_v(K)]$$

$$\times A_1A_2(J, L)N(J, K)\int \rho\rho\, da.$$

The sum over L includes all azimuth bins that correspond to depths included in the depth bin K.

The effective geometrical factor for pairs adjusted for the range of depths in the depth bin K is then

$$A_1A_2(J, K) = \sum_L [I_v(h\to L)/I_v(K)]A_1A_2(J, L).$$

In a similar way, the effective geometrical factor for triples is given by

$$A_1A_2A_3(J, K) = \sum_L [I_v(h\to L)/I_v(K)]A_1A_2A_3(J, L).$$

---

*Research supported by the National Science Foundation.

[1]J. A. Anderson, O. I. Dahl, T. B. Day, J. H. Friedman, J. Kirz, L. H. Schmidt, R. J. Sprafka, and M. A. Wahlig, LRL Report No. UCRL-17366, 1967 (unpublished).

[2]P. L. Connolly, W. E. Ellis, P. V. C. Hough, D. J. Miller, T. W. Morris, C. Ouannes, R. S. Panvini, and A. M. Thorndike, in *Proceedings of the Topical Conference on High-Energy Collisions of Hadrons, CERN, 1968* (CERN, Geneva, 1968).

[3]Y. Pal and B. Peters, Kgl. Danske Videnskab. Selskab, Mat.-Fys. Medd. 33, No. 15 (1964).

[4]G. Cocconi, L. J. Koester, and D. H. Perkins, LRL Report No. UCRL-10022, 1961 (unpublished); G. Cocconi, Phys. Rev. 111, 1699 (1958).

[5]O. Cryzewski, in *Proceedings of the Topical Conference on High-Energy Collisions of Hadrons, CERN, 1968,* Ref. 2.

[6]V. S. Barashenkov and V. M. Maltsev, Fortschr. Physik 15, 435 (1967).

[7]Y. Fujimoto and S. Hayakawa, *Handbuch der Physik,* edited by S. Flügge (Springer, Berlin, 1967).

[8]M. Koshiba, Rapporteur talk in the *Tenth International Conference on Cosmic Rays, Calgary, Alberta, Canada, 1967,* edited by R. J. Prescott (University of Calgary, Alberta, Canada, 1967), Pt. A.

[9]H. Pilkuhn, Rapporteur talk in the *Proceedings of the Topical Conference on High-Energy Collisions of Hadrons, CERN, 1968,* Ref. 2.

[10]K. Greisen, in *Proceedings of the Ninth International Conference on Cosmic Rays, 1965,* edited by A. C. Stickland (The Institute of Physics and the Physical Society, London, England, 1966), Vol 2; J. Trumper, in *Proceedings of the Eleventh International Conference on Cosmic Rays, Budapest, 1969,* edited by P. Gombás, Acta

Phys. Acad. Sci. Hung. Suppl. 2, 497 (1970).

[11]P. H. Barrett, L. M. Bollinger, G. Cocconi, Y. Eisenberg, and K. Greisen, Rev. Mod. Phys. 24, 133 (1952).

[12]B. K. Chatterjee, S. Lal, T. Matano, G. T. Murthy, S. Naranan, K. Sivaprasad, B. V. Sreekantan, M. V. Srinivasa Rao, and P. R. Vishwanath, in *Proceedings of the Ninth International Conference on Cosmic Rays, 1965,* edited by A. C. Stickland, Ref. 10.

[13]L. G. Porter and R. O. Stenerson, J. Phys. A 2, 374 (1969).

[14]H. E. Bergeson and C. J. Wolfson, Nucl. Instr. Methods 51, 47 (1967); L. K. Hilton, M. L. Morris, and R. O. Stenerson, *ibid.* 51, 43 (1967); J. W. Keuffel and J. L. Parker, *ibid.* 51, 29 (1967); H. E. Bergeson, J. W. Keuffel, M. O. Larson, E. R. Martin, and G. W. Mason, Phys. Rev. Letters 19, 1487 (1967); H. E. Bergeson, J. W. Keuffel, M. O. Larson, G. W. Mason, and J. L. Osborne, *ibid.* 21, 1093 (1968); J. W. Keuffel, in Proceedings of the Utah Academy of Sciences 45, Part I, 1968 (unpublished); S. C. Barrowes, H. E. Bergeson, R. B. Coats, J. W. Keuffel, M. O. Larson, J. L. Osborne, S. Ozaki, and R. O. Stenerson, in *Proceedings of the Eleventh International Conference on Cosmic Rays, Budapest, 1969,* edited by P. Gombás, Acta Phys. Acad. Sci. Hung. Suppl. 1, 445 (1970); H. E. Bergeson, G. L. Bolingbroke, J. W. Keuffel, M. O. Larson, G. H. Lowe, G. W. Mason, J. H. Parker, J. L. Osborne, and R. O. Stenerson, *ibid.* 2 (1970); H. E. Bergeson, R. B. Coats, J. W. Keuffel, M. O. Larson, G. H. Lowe, J. L. Osborne, S. Ozaki, J. H. Parker, R. O. Stenerson, *ibid.* 2 (1970); H. E. Bergeson, G. L. Bolingbroke, D. E. Groom, J. W. Keuffel, and J. L. Osborne, in *Proceedings of the Fifteenth International Conference on High-Energy Physics, Kiev, U.S.S.R., 1970* (Atomizdat, Moscow, to be published); H. E. Bergeson, G. H. Lowe, G. W. Mason, S. Ozaki, and D. M. Price, Bull. Am. Phys. Soc. 15, 1619 (1970).

[15]A. E. Bussian, G. D. De Meester, L. W. Jones, B. W. Loo, D. E. Lyon, P. V. R. Murthy, and R. F. Roth, Phys. Rev. Letters 25, 1679 (1970).

[16]H. H. Aly, M. F. Kaplon, and M. L. Shen, Nuovo Cimento 31, 905 (1964); E. W. Anderson, E. J. Bleser, R. A. Carrigan, G. B. Collins, R. M. Edelstein, T. Fujii, N. C. Hien, T. J. McMahon, J. Menes, I. Nadelhaft, and F. Turkot, Phys. Rev. Letters 16, 855 (1966); 19, 198 (1967); E. W. Anderson and G. B. Collins, *ibid.* 19, 201 (1967); J. G. Asbury, D. G. Crabb, J. L. Day, A. D. Krisch, M. T. Lin, M. L. Marshak, L. G. Ratner, and A. L. Read, *ibid.* 21, 1097 (1968); Y. Y. Chen, J. W. Elbert, A. R. Erwin, S. Mikamo, D. Reeder, W. D. Walker, and A. Weinberg, in *Proceedings of the Topical Conference on High-Energy Collisions of Hadrons, CERN, 1968,* Ref. 2; C. W. Akerlof, D. G. Crabb, J. L. Day, K. W. Edwards, A. D. Krisch, M. T. Lin, and L. G. Ratner, Phys. Rev. 166, 1353 (1968).

[17]C. Adcock, J. Wdowczyk, and A. W. Wolfendale, J. Phys. A 2, 574 (1969); C. Adcock, R. B. Coats, J. Wdowczyk, and A. W. Wolfendale, *ibid.* 3, 697 (1970); J. F. de Beer, B. Holyoak, J. Wdowczyk, and A. W. Wolfendale, Proc. Phys. Soc. (London) 89, 657 (1966).

[18]H. E. Bergeson, R. B. Coats, J. W. Keuffel, M. O. Larson, G. H. Lowe, J. L. Osborne, S. Ozaki, J. H. Parker, and R. O. Stenerson, J. Phys. A 3, 689 (1970); H. E. Bergeson, R. B. Coats, J. W. Keuffel, M. O. Larson, S. Ozaki, and R. O. Stenerson, in *Proceedings of the Eleventh International Conference on Cosmic Rays, Budapest 1969,* Ref. 10.

[19]T. M. Cannon and R. O. Stenerson, J. Phys. A 4, 266 (1971).

[20]E. N. Parker, in *Dynamical Properties of Cosmic Rays, Stars and Stellar Systems, Vol VII: Nebulae and Interstellar Matter,* edited by B. M. Middlehurst and L. H. Aller (Univ. of Chicago Press, Chicago, 1968), Chap. 14.

[21]G. Buckwalter, C. Cowan, and D. Ryan, in *Proceedings of the Ninth International Conference on Cosmic Rays, 1965,* edited by A. C. Stickland, Ref. 10.

[22]J. C. Barton, J. P. Betts, and C. M. Pourgides, in Proceedings of the Sixth Inter-American Seminar on Cosmic Rays, La Paz, 1970 (unpublished).

[23]R. M. Jacklyn, in *Proceedings of the Ninth International Conference on Cosmic Rays, 1965,* edited by A. C. Stickland, Ref. 10; R. M. Jacklyn, Nature 211, 690 (1966).